Dynamical Study of Surge Behavior in Axial Flow Compressors

Der-Cherng Liaw, Li-Feng Tsai

Abstract—**It is known that two types of unstable phenomena might occur while the compressor operates near its maximum achievable pressure rise. Those might limit the operation of gas turbine jet engines. Under either one of the two unstable conditions, a moderate disturbance can result in system instability so that the compression system might either experience a large amplitude oscillation (corresponding to the so-called "surge") or jump into a very inefficient operation at constant mass flux and low pressure-rise (corresponding to the so-called "stall"). In a previous study (Liaw and Abed, 1996), we had presented the study of stall behaviour in axial flow compressors by using Moore-Greitzer's model proposed in 1986. Not only the condition for the occurrence of stall wave was derived, a quadratic type control law was also proposed to prevent the appearance of stall in compressor dynamics. In this paper, we extend those results to focus on the study of surge behaviour by using the same model without considering the dynamics of stall wave. Conditions for local stability and non-local dynamical behavior of axial flow compressor are analytically obtained by using system linearization and bifurcation theorem. Numerical results will also be presented to show the linkage between bifurcation phenomena and system instabilities.**

***Index Terms*—Axial flow compressor, bifurcation, stability.**

I. INTRODUCTION

In the recent years, it has attracted lots of attention in the study of axial flow compressor. One of the major reasons is that the flow can become unstable when an axial flow compressor operates close to its maximum achievable pressure-rise. Those instabilities put a large stress on the engine, and in some cases the engine needs to turn off in order to recover back to the original operation [1]. Among them, there are two primary types of instabilities that occur in the flow through the axial flow compressor. One is the so-called "surge," which is commonly characterized by large-amplitude oscillations of the flow through the compressor. During part of the cycle, the mean mass flow may become reversed, thrusting air out from the front end of the engine. This puts a large stress on the components of the engine and seriously impairs system. The other is the so-called "rotating stall," which is corresponding to a travelling wave of gas around the annulus of the compressor and results in a very inefficient operation at constant mean mass flow rate and low pressure rise [2]. Both rotating stall and surge behavior can reduce the pressure rise in the compressor, cause rapid heating of blades, and might induce severe mechanical distress.

In 1986, Moore and Greitzer [1] extended the results of [3] and proposed a third-order differential equation model to describe both surge and rotating stall phenomena occurring in axial flow compression systems. That model incorporates asymmetric dynamics, while employing an axisymmetric steady-state compressor characteristic. Based on Moore and Greitzer's model [1], the stall behavior of axial flow compression system was found to be attributed to the appearance of the so-called "transcritical bifurcation" [4] or the so-called "pitch-fork bifurcation" [5] depending on the representation of system state. In practical applications, a surge (or stall) line is usually drawn to provide a safe operational boundary for the usage of compressors. Such a conservative trade-off unduly restricts the capability of engine. Various control methods have been recently proposed to allow compressors to operate safely beyond the surge line and thus enhance system efficiency (e.g., [6]-[13]). It is known that the unstable portion of the compressor's axisymmetric characteristic is hard to measure and the associated system uncertainties are inevitable in practical applications [6]-[7]. Robust control schemes had been applied to deal with such uncertainties by assuming the axisymmetric characteristic to be a specific cubic function [10]-[11].

In this paper, we will extend the results of [5] to focus on the study of surge behaviour by using the same model without considering the dynamics of stall wave. A preliminary result of this study had been presented in [16] via extensive computer simulations and numerical continuation code AUTO [14]-[15] for the axial flow compressor dynamics with respect to the variations of both parameters γ and B. Phase portraits were also constructed in [16] by simulation to illustrate the distinctly-different dynamical behaviours associated with each regime on system parameter space. Instead of using numerical approach only as that in [16], in this study we focus on both of the local stability analysis and local bifurcation analysis for the compression systems via system linearization and bifurcation theory by treating γ as system parameter. The numerical continuation and bifurcation analysis package AUTO [14]-[15] will also be employed to evaluate the systems dynamical behavior with respect to the variation of the so-called "B-parameter" [3] and the value of the throttle setting for justifying the analytical results.

The paper is organized as follows. In Section II, we first recall the Andronov-Hopf bifurcation theorem which will then be used in Section III to derive the conditions for the occurrence of surge behavior. A brief review of the system models for compressor dynamics and analytical results for the study of rotating stall are also given. It is followed by the

D.-C. Liaw, Institute of Electrical and Control Engineering, National Yang Ming Chiao Tung University, 1001 Ta Hsueh Road, Hsinchu, Taiwan, R.O.C.

L.-F. Tsai, Institute of Electrical and Control Engineering, National Yang Ming Chiao Tung University, 1001 Ta Hsueh Road, Hsinchu, Taiwan, R.O.C.

analysis of local stability and possible bifurcation of a reduced version of Moore and Greitzer's model via system linearization scheme and bifurcation theorem. The linkage between local bifurcation and surge behavior in compressor will be discussed in Section IV by using numerical approach. Finally, Section V gives the main conclusions.

Notation:

A amplitude of the first angular mode of rotating stallwave;
$\dot{m}_C$ nondimensional compressor mass flow rate;
ΔP nondimensional plenum pressure rise;
θ angle along circumference;
α a geometry-related constant;
W semi-width of cubic characteristic
C_{ss} nondimensional axisymmetric compressor characteristic;
F inverse function of nondimensional throttle pressure rise;
B Greitzer B parameter, proportional to rotor speed and plenum volume;
γ control parameter of throttle function;

II. Preliminaries

In this section, we will briefly review basic concepts of Andronov-Hopf bifurcation theorem and the mathematical model of axial flow compressor dynamics which will then be used in the sequel.

A. Andronov-Hopf Bifurcation

First, we recall the results of Andronov-Hopf bifurcation theorem from (e.g., [17]) as follows.

Consider one-parameter families of nonlinear ordinary differential equations as given by

$$\dot{x} = f(x,\mu), \tag{1}$$

where $x \in R^n$, $\mu \in R$ and f is a smooth function. Assume $(x,\mu)=(0,0)$ is an equilibrium point of system (1). The Taylor series expansion of Eq. (1) with respect to both the state variable x and the bifurcation parameter μ at the equilibrium point $(x,\mu)=(0,0)$ can then be obtained as given by

$$\dot{x} = L_0 x + Q_0(x,x) + C_0(x,x,x) + \cdots + \mu(L_1 x + Q_1(x,x) + C_1(x,x,x) + \cdots) + \mu^2(L_2 x + Q_2(x,x) + C_2(x,x,x) + \cdots) + \cdots \tag{2}$$

Here, $Q_k(x,x) \triangleq \frac{1}{2!k!} D_{\mu^k xx} f(x,\mu), C_k(x,x,x) \triangleq \frac{1}{3!k!} D_{\mu^k xxx} f(x,\mu)$ denote the bi-linear and tri-linear parts of $f(x,\mu)$, respectively, $L_0 \triangleq D_x f(0,0)$ is the Jacobian matrix and $L_k \triangleq \frac{1}{k!} D_{\mu^k x} f(0,0)$.

Suppose the Jacobian matrix L_0 possess a pair of pure imaginary eigenvalues $\pm i\omega_c$. Denote l and r the corresponding left and right eigenvectors of L_0 for the eigenvalue $i\omega_c$. Here, for the simplification of calculation, the first component of r is set to 1 and the left eigenvector l is chosen so that $l \cdot r = 1$. We then have the following result from [17].

Lemma 1. System (1) will exhibit Andronov-Hopf bifurcation at the equilibrium point $(x,\mu)=(0,0)$ if (i) the Jacobian matrix L_0 possess a pair of pure imaginary eigenvalues $\pm i\omega_c$ and (ii) $\Re e\{lL_1 r\} \neq 0$. Here, $\Re e\{\cdot\}$ denotes the real part of the value. Moreover, the induced periodic solutions emerging from the equilibrium point (or the so-called "Andronov-Hopf bifurcation point") is orbitally asymptotically stable (resp. unstable) if $\beta_2 < 0$ (resp. if $\beta_2 > 0$), where

$$\beta_2 = 2 \cdot \Re e\left\{ 2lQ_0(r,a) + l\left[Q_0(\bar{r},b) + \frac{3}{4} C_0(r,r,\bar{r}) \right] \right\}$$

with a and b satisfying the following two relations:

$$-L_0 a = \frac{1}{2} Q_0(r,\bar{r})$$

and

$$(2i\omega_c I - L_0) b = \frac{1}{2} Q_0(r,r)$$

Here, bar denotes the complex conjugate.

B. Axial Flow Compressor Dynamics

Conceptually, a compression system is mainly consisted of inlet duct, compressor, exit duct, plenum, and throttle. A third-order ordinary differential equation model was proposed by Moore and Greitzer in 1986 [1] to capture the most essential features of compressor dynamics. To adopt the notations of Liaw and Abed [5], the proposed model in [1] can be represented as

$$\frac{dA}{dt} = \frac{\alpha}{\pi W} \int_0^{2\pi} C_{ss}(\dot{m}_C + WA\sin\theta)\sin\theta \, d\theta, \tag{3}$$

$$\frac{d\dot{m}_C}{dt} = -\Delta P + \frac{1}{2\pi} \int_0^{2\pi} C_{ss}(\dot{m}_C + WA\sin\theta) \, d\theta, \tag{4}$$

$$\frac{d\Delta P}{dt} = \frac{1}{4B^2} \{ \dot{m}_C - F(\gamma, \Delta P) \}. \tag{5}$$

In the system dynamics given in (3)-(5) above, Eq. (4) is obtained from momentum balance and implies that the acceleration of the fluid in the inlet ducts is proportional to the difference between the pressure-rise across the compressor and the pressure rise in the plenum. The variable of integration θ represents the angular displacement from a reference stationary with the first harmonic mode of the stall wave. In addition, Eq. (3) governs the rate of the amplitude $A(t)$ and Eq. (5) determines the changing rate of the plenum pressure. The inverse function of nondimensional throttle pressure rise is usually taken as

$$F(\gamma, \Delta P) = \gamma(\Delta P)^{1/2}. \tag{6}$$

It is known that the axisymmetric compressor characteristic $C_{ss}(\cdot)$ characterizes the steady pressure rise across the compressor and is often an S-shaped function (e.g., a cubic polynomial in [4]-[5]). An example is depicted in Fig. 1.

Assume $C_{SS}(\cdot)$ is a smooth function. We can then solve for the equilibrium points of system (3)-(5). It is not difficult to find that $A=0$ results in dA/dt =0 in (3). Denote $x^0 = (0, \dot{m}_C^0, \Delta P^0)$ as an equilibrium point for the system (3)-(5). It is observed from Eqs. (4)-(5) that we will have $\Delta P^0 = C_{ss}(\dot{m}_C^0)$ and $\dot{m}_C^0 = F(\gamma^0, \Delta P^0)$ for $A=0$ with a given $\gamma = \gamma^0$. That means system equilibrium will be at the intersection point of the throttle line and the compressor characteristic for $A=0$. Note that, there may have equilibrium points of system (3)-(5) for $A \neq 0$, which corresponds to the so-called "stall behavior." To adopt the

results from [5], it is observed in Fig. 1 that the throttle line intersects the compressor characteristic at a unique point while the throttle is widely open (i.e., the value of system parameter γ is large). On the other hand, the equilibrium mass flow will decrease while the value of γ is getting smaller. As depicted in Fig. 1, a dot-line stands for unstable system equilibria while solid line stands for stable ones. The conditions for the local stability and the existence for the occurrence of stall (i.e., $A \neq 0$) had been obtained in [5] as recalled below.

Lemma 2. Suppose F is a strictly increasing function in each of its two variables. Then the equilibrium point x^0 of system (3)-(5) is asymptotically stable if $C'_{ss}(\dot{m}_C^0(\gamma)) < 0$, while it is unstable for $C'_{ss}(\dot{m}_C^0(\gamma)) > 0$.

Lemma 3. Suppose F is a strictly increasing function in each of its two variables with $C'_{ss}(\dot{m}_C^0(\gamma)) = 0$ and $C''_{ss}(\dot{m}_C^0(\gamma)) \neq 0$. Then the system (3)-(5) will exhibit a pitchfork stationary bifurcation at the equilibrium point x^0 with respect to small variation of γ.

Note that, the stability conditions for the bifurcated solutions were obtained in [5] while a quadratic type control law was also proposed to prevent the appearance of stall in compressor dynamics.

III. Dynamical Analysis

In this paper, we will extend the results of [5] to focus on the study of surge behaviour by using the same model as presented in above Eqs. (3)-(5) without considering the dynamics of stall wave. A preliminary result of this study was presented in [16] by using extensive computer simulations and numerical continuation code AUTO [14]-[15] for the axial flow compressor dynamics with respect to the variations of both parameters γ and B. Instead of using numerical approach only as those in [16], in the following we focus on both of the local stability analysis and bifurcation analysis for the compression systems via bifurcation theory by treating γ as system parameters. Details are given below.

A. Local Stability Analysis

It is known that the so-called "surge behaviour" is a dynamic instability, which occurs when the compressor feeds more mechanical energy than the rest of the system can dissipate. That results in an oscillatory disturbance growing exponentially until it is limited by nonlinearity effects and becomes a limit cycle [17].

As discussed in [5], the operating points lying on both normal un-stalled zone and pre-stall zone as depicted solid curve of $C_{ss}(\cdot)$ in Fig. 1 will be always stable. That leads to the fact that the surge behavior will only appear at the operating point which is on the unstable portion of $C_{ss}(\cdot)$. It is observed from Eq. (3) that A=0 is an invariant manifold for system (3)-(5). Thus, Eqs. (3)-(5) can then be reduced as a two-dimensional system for the study of surge behaviour as given below (with A=0):

$$\frac{d\dot{m}_C}{dt} = C_{ss}(\dot{m}_C) - \Delta P, \tag{7}$$

$$\frac{d\Delta P}{dt} = \frac{1}{4B^2}\{\dot{m}_C - F(\gamma, \Delta P)\}. \tag{8}$$

First, we study the local stability of system (7)-(8). Let $x^0 = \left(\dot{m}_c^0, \Delta P^0\right)^T$ be an equilibrium point of system (7)-(8) at $\gamma = \gamma^0$ with $\Delta P^0 = C_{ss}(\dot{m}_C^0)$ and $\dot{m}_C^0 = F(\gamma^0, \Delta P^0)$. Denote $x = (x_1, x_2)^T$ with $x_1 = \dot{m}_c - \dot{m}_c^0$ and $x_2 = \Delta P - \Delta P^0$. The linearization of system (7)-(8) at the equilibrium x^0 gives

$$\dot{x} = L_0 x, \tag{9}$$

with

$$L_0 = \begin{pmatrix} C'_{ss}(\dot{m}_C^0) & -1 \\ \frac{1}{4B^2} & -\frac{1}{4B^2}F'\left(\gamma^0, \Delta P^0\right) \end{pmatrix}. \tag{10}$$

Here, $F'\left(\gamma^0, \Delta P^0\right)$ denotes the slope of the throttle line at $(\dot{m}_C^0, \Delta P^0)^T$ and $C'_{ss}(\dot{m}_C^0)$ is the slope of the compressor curve at $(\dot{m}_C^0, \Delta P^0).^T$

The characteristic equation of the linearized model (9) is obtained as

$$\lambda^2 + \{\frac{1}{4B^2}F'(\gamma^0, \Delta P^0) - C'_{SS}(\dot{m}_C^0)\}\lambda + \frac{1}{4B^2}\{1 - F'(\gamma^0, \Delta P^0)C'_{SS}(\dot{m}_C^0)\} = 0. \tag{11}$$

Suppose B >0 and F is a strictly increasing function, i.e., $F'\left(\gamma^0, \Delta P^0\right) > 0$. Then from the Routh-Hurwitz criterion, we have the following stability results at $(\dot{m}_C^0, \Delta P^0)^T$.

Lemma 4. The equilibrium point $x^0 = \left(\dot{m}_c^0, \Delta P^0\right)^T$ of system (7)-(8) is asymptotically stable (resp. unstable) if $C'_{ss}\left(\dot{m}_c^0\right) < min\left\{1/F'\left(\gamma^0, \Delta P^0\right), \frac{1}{4B^2}F'\left(\gamma^0, \Delta P^0\right)\right\}$ (resp. if $C'_{ss}\left(\dot{m}_c^0\right) > min\left\{1/F'\left(\gamma^0, \Delta P^0\right), \frac{1}{4B^2}F'\left(\gamma^0, \Delta P^0\right)\right\}$).

B. Local Bifurcation

From Eq. (11), system (7)-(8) renders to the critical system if the real part of either of two eigenvalues equals to zero. From bifurcation theory [17], we know that bifurcation may occur at which the parameter-dependent system becomes critical. A particular bifurcation sometimes is associated with surge, for instance, the Andronov-Hopf bifurcation, of which a periodic solution emerges from an equilibrium point as system parameters varying. The existence conditions for the appearance of Andronov-Hopf bifurcation theorem as recalled in Section II are that a pair of eigenvalues of the system linearization will cross the imaginary axis transversely at a critical value of the parameter. It is observed from Lemma 4 that the key parameter in this model for determining the nature of post-instability compressor behavior (surge) is the value of B-parameter.

From the characteristic equation as in (11), we find that the linearization of system (7)-(8) has a pair of pure imaginary

eigenvalues if $1/F'\left(\gamma^0,\Delta P^0\right) > C'_{SS}(\dot{m}_C^0) > 0$ with the value of $B(:=B_H)=\sqrt{F'\left(\gamma^0,\Delta P^0\right)/4C'_{ss}\left(\dot{m}_c^0\right)}$. This implies that an Andronov-Hopf bifurcation may occur from the equilibrium point x^0 for some value of $\gamma=\gamma^0$. To analyze such a possibility, we will employ the result recalled in Lemma 1 as given above. That result can help to derive the conditions for the existence and stability of an Andronov- Hopf bifurcation from the nominal system equilibrium.

Let x^0 be the equilibrium point at which the linearization of system (7)-(8) has a pair of pure imaginary eigenvalues $\pm i\omega_c$ for some $\gamma=\gamma^0$. The Taylor series expansion of system (7)-(8) for (x,γ) near (x^0,γ^0) is given by

$$\dot{x}=L_0x+Q_0(x,x)+C_0(x,x,x)+\left(\gamma-\gamma^0\right)L_1x+\cdots \tag{12}$$

Here, L_0 is as in (10) and

$$Q_0(x,x)=\begin{pmatrix}\frac{1}{2}C''\left(\dot{m}_c^0\right)x_1^2\\ -\frac{1}{8B^2}F''\left(\gamma^0,\Delta P^0\right)x_2^2\end{pmatrix}, \tag{13}$$

$$C_0(x,x,x)=\begin{pmatrix}\frac{1}{6}C'''_{ss}\left(\dot{m}_c^0\right)x_1^3\\ -\frac{1}{24B^2}F'''\left(\gamma^0,\Delta P^0\right)x_2^3\end{pmatrix} \tag{14}$$

$$L_1=\begin{pmatrix}C''_{ss}\left(\dot{m}_c^0\right)\phi_1 & 0\\ 0 & -\frac{1}{4B^2}\phi_2\end{pmatrix}, \tag{15}$$

where $\phi_1=\frac{\partial F}{\partial\gamma}\left(\gamma^0,\Delta P^0\right)$ and $\phi_2=\frac{\partial^2F}{\partial\gamma\partial\Delta P}\left(\gamma^0,\Delta P^0\right)$.

After some algebraic derivation, the left and right eigenvectors of L_0 with eigenvalue $i\omega_c$ are chosen as $l=\left(\frac{1}{2}-\frac{C'_{ss}\left(\dot{m}_c^0\right)}{2\omega_c}i,\ \frac{1}{2\omega_c}i\right)$ and $r=\left(1,\ C'_{ss}\left(\dot{m}_c^0\right)-i\omega_c\right)^T$.

Here, $\omega_c=\frac{1}{2B}\sqrt{1-F'\left(\gamma^0,\Delta P^0\right)C'_{ss}\left(\dot{m}_c^0\right)}$. To check the transversality condition $\Re e\{lL_1r\}\neq 0$ as recalled in Lemma 1, we have

$$lL_1r=\frac{1}{2}\{C''_{ss}\left(\dot{m}_c^0\right)\phi_1-\frac{1}{4B^2}\phi_2\}-i\frac{C'_{ss}\left(\dot{m}_c^0\right)}{2\omega_c}\{C''_{ss}\left(\dot{m}_c^0\right)\phi_1+\frac{1}{4B^2}\phi_2\}$$

(16)

From Lemma 1, the property of Andronov-Hopf bifurcation can be characterized by the bifurcation coefficient β_2 as: (i) $\beta_2<0$, then the system has supercritical Andronov-Hopf bifurcation which implies the bifurcated oscillation is stable; and (ii) $\beta_2>0$, the system has subcritical Andronov-Hopf bifurcation which implies the bifurcated oscillation is unstable.

After some calculation, we have *a* and *b* from Lemma 1 as

$$a=\frac{1}{4\Delta}\begin{pmatrix}a_1\\ a_2\end{pmatrix} \tag{17}$$

and $b=\frac{1}{3\Delta}\begin{pmatrix}b_{11}+b_{12}i\omega_c\\ \frac{1}{4}\left(b_{21}+b_{22}i\omega_c\right)\end{pmatrix}$, (18)

where

$$\Delta=1-F'\left(\gamma^0,\Delta P^0\right)C'_{ss}\left(\dot{m}_c^0\right), \tag{19}$$

$$a_1=F'\left(\gamma^0,\Delta P^0\right)C''_{ss}\left(\dot{m}_c^0\right)+\frac{1}{4B^2}F''\left(\gamma^0,\Delta P^0\right), \tag{20}$$

$$a_2=C''_{ss}\left(\dot{m}_c^0\right)+\frac{1}{4B^2}C'_{ss}\left(\dot{m}_c^0\right)F''\left(\gamma^0,\Delta P^0\right) \tag{21}$$

$$b_{11}=\frac{1}{16B^2}F''\left(\gamma^0,\Delta P^0\right)-\frac{1}{2}F''\left(\gamma^0,\Delta P^0\right)\left(C'_{ss}\left(\dot{m}_c^0\right)\right)^2-B^2C'_{ss}\left(\dot{m}_c^0\right)C''_{ss}\left(\dot{m}_c^0\right), \tag{22}$$

$$b_{12}=\frac{1}{2}F''\left(\gamma^0,\Delta P^0\right)C'_{ss}\left(\dot{m}_c^0\right)-2B^2C''_{ss}\left(\dot{m}_c^0\right), \tag{23}$$

$$b_{21}=F''\left(\gamma^0,\Delta P^0\right)\{\frac{5}{4B^2}C'_{ss}\left(\dot{m}_c^0\right)-6\left(C'_{ss}\left(\dot{m}_c^0\right)\right)^3\}-C''_{ss}\left(\dot{m}_c^0\right) \tag{24}$$

$$b_{22}=F''\left(\gamma^0,\Delta P^0\right)\{6\left(C'_{ss}\left(\dot{m}_c^0\right)\right)^2-\frac{1}{2B^2}\}. \tag{25}$$

The bifurcation coefficient β_2 for system (7)-(8) is then obtained from Lemma 1 as below:

$$\beta_2=\frac{1}{8\Delta}\{F'\left(\gamma^0,\Delta P^0\right)\left(C''_{ss}\left(\dot{m}_c^0\right)\right)^2-\frac{1}{16B^4}\left(F''\left(\gamma^0,\Delta P^0\right)\right)^2\cdot C'_{ss}\left(\dot{m}_c^0\right)\}-\frac{1}{128B^4}F'''\left(\gamma^0,\Delta P^0\right)+\frac{1}{8}C'''_{ss}\left(\dot{m}_c^0\right). \tag{26}$$

To conclude the discussion above, we have the next result.

Theorem 1. Assume $1/F'\left(\gamma^0,\Delta P^0\right) > C'_{SS}(\dot{m}_C^0) > 0$. Then system (7)-(8) will exhibits Andronov-Hopf bifurcation at the equilibrium point $(\dot{m}_C^0,\Delta P^0)^T$ if $C''_{ss}\left(\dot{m}_c^0\right)\phi_1-\frac{1}{4B^2}\phi_2$ and $B=\sqrt{F'\left(\gamma^0,\Delta P^0\right)/4C'_{ss}\left(\dot{m}_c^0\right)}$. Moreover, the bifurcated periodic solution is stable (resp. unstable) if $\beta_2<0$ (resp. if $\beta_2>0$), where β_2 is given in (26).

IV. Illustrative Example

In the following, we will adopt the cubic model from [6] as given in (12) below for numerical analysis to verify the local results of Lemma 4 and Theorem 1.

$$C_{ss}(\dot{m}_C)=1.56+1.5(\dot{m}_C-1)-0.5(\dot{m}_C-1)^3. \tag{27}$$

As discussed in Section II, the Moore and Greitzer's model [1] is mainly used to describe the dynamics of rotating stall. As recalled in Lemma 2, the linear stability of the axisymmetric equilibrium is stable (resp. unstable) for $C'_{ss}(\dot{m}_C^0(\gamma))<0$ (resp. $C'_{ss}(\dot{m}_C^0(\gamma))>0$). From nonlinear system point of view, however, the domain of attraction for stable system equilibrium may vary as the value of system parameters γ and *B*. change. When the domain of attraction becomes finite, shrinks and disappears, emergences of multi-equilibria and/or limit-cycle type of oscillations may occur. In the following, the

numerical analysis tool AUTO [15] is employed to unveil a series of possible nonlinear phenomena.

As presented in [5], the whole operating regime of the compression system (3)-(5) can be divided into three regimes as depicted in Fig. 1 via the different setting value of the throttle. They are: (i) the un-stalled normal zone for $\gamma > \gamma_s$, (ii) the pre-stall zone for $\gamma_s \geq \gamma \geq \gamma_c$, and (iii) the stall zone for $\gamma < \gamma_c$, of which $\gamma_c = 1.25$ and $\gamma_s = 1.463$. Two-parameter bifurcation diagram for the system (7)-(8) is obtained by using code AUTO as given in Fig. 2. In that figure, yellow-line ($\gamma = 1.25$) and pink-line ($\gamma = 1.463$) stand for the throttle values which separate the operational regime of compressor into three zones as shown in Fig. 1. In addition, blue-line stands for Andronov-Hopf bifurcation points for the system (7)-(8). Detailed discussions of system dynamics in each of three major zones are given as follows.

First, we consider the dynamical behavior in the un-stalled normal zone. As depicted in Fig. 2, no bifurcation is found in that region. A typical time response is shown in Fig. 3 for the setting value of $\gamma = 1.6$ and $B = 0.5$, which denotes the point *A* in Fig. 2. It is clear that the equilibrium point for both of two-dimensional system (7)-(8) and third-order system (3)-(5) are stable. In Fig. 3, the pink dotted-dashed line denotes the time response for the third-order system (3)-(5) with initial $A = 0.5$, while the blue dotted-dashed line denotes the time response for the two-dimensional system (7)-(8) with initial $A = 0$, respectively. Note that, the definitions for the two time response curves will also be applied to the numerical simulations presented below.

Next, we consider the case of which the equilibrium point lying on the pre-stall zone with $\gamma = 1.3$. Time responses for both of small and large values for *B*-parameter are obtained in Figs. 4-7. Here, we choose $B = 0.5$ and $B = 2$ denoted as points B and C in Fig. 2 for the numerical study. Similar scenarios as those in the un-stalled normal zone are observed in Figs. 4-7 to show the stability of the high pressure equilibrium point. The main difference between the dynamical behaviors of two system models is that the equilibrium lying on the pre-stall zone is not a unique one for the third-order system (3)-(5). It is clear to see in Figs. 5 and 7 that trajectories for $A = 0.5$ with system initials close to low pressure equilibrium point will go to the low pressure equilibrium point instead of the high pressure equilibrium point. In addition, as depicted in Fig. 6 that both of time responses for the system (7)-(8) and the third-order system (3)-(5) will pass through a short period of deep-surge alike behavior and then approach the high pressure equilibrium point.

Based on the numerical results presented above, we can conclude that no surge behavior is observed for the compressor dynamics with equilibrium point lying on either un-stalled normal zone or pre-stall zone.

Now, we consider the case of which the equilibrium point lying on the stall zone with $\gamma = 1.13$. Time responses for four different values for *B*-parameter are obtained in Figs. 8-11. Here, we choose $B = 0.2,\ 0.3942,\ 0.5$ and 1.5 denoted as four points D, E, F and G in Fig. 2 for the numerical study. As derived in Section III, the Andronov-Hopf bifurcation might appear while the equilibrium point lies on the positive slope of the axisymmetric compressor characteristic, i.e., $C'_{ss}(\dot{m}_C^0) > 0$, and the conditions of Theorem 1 hold. As shown in Figs. 8-11, we have different scenarios for time response as the value of B-parameter changes. Detailed are summarized as follows:

(i) When the value of *B*-parameter is small, e.g., $B = 0.2$, no Andronov-Hopf bifurcation will occur. As shown in Fig. 8, the transients settle on the stable low pressure stalled equilibrium for system (3)-(5) and the high pressure equilibrium point for (7)-(8) with initials $A = 0.5$ and $A = 0$, respectively.

(ii) When the value of *B*-parameter is increased to a moderate value e.g., $B = 0.3492$, as depicted in Fig. 9 the system (7)-(8) exhibits Andronov-Hopf bifurcation for the initial with $A = 0$ and the transient with $A = 0.5$ settles on the stable low pressure stalled equilibrium for system (3)-(5), respectively. To check the conditions given in Theorem 1 with $\gamma = 1.13$, we have the equilibrium point for system (7)-(8) as $(\dot{m}_C^0, \Delta P^0) = (1.7852,\ 2.4957)$. We then have the first derivatives $F'\left(\gamma^0, \Delta P^0\right) = 0.3576$, $C'_{ss}\left(\dot{m}_C^0\right) = 0.5753$ with $B = \sqrt{F'\left(\gamma^0, \Delta P^0\right) / 4C'_{ss}\left(\dot{m}_C^0\right)} = 0.3942$. The so-called "transversality condition" for the bifurcation is calculated as $C''_{ss}\left(\dot{m}_c^0\right)\phi_1 - \frac{1}{4B^2}\phi_2 = -4.23 \neq 0$, while the bifurcation coefficient is obtained as $\beta_2 = -0.0778 < 0$. Numerical simulation depicted in Fig. 9 agrees with the results implied by Theorem 1.

(iii) As the value of *B*-parameter increases a little bit, say, $B = 0.5$, as depicted in Fig. 10 the amplitude of oscillation for the system (7)-(8) becomes larger to form the so-called "surge" behavior. However, the transient with $A = 0.5$ still settles on a stable low pressure stalled equilibrium for system (3)-(5).

(iv) As the value of *B*-parameter becomes larger, say, $B = 1.5$, the amplitude of oscillation for the system (7)-(8) eventually forms the so-called "deep-surge" as shown in Fig. 12. It is interesting to note that the transient with $A = 0.5$ for system (3)-(5) will also go to the deep-surge instead of settling on the stable low pressure stalled equilibrium.

V. Conclusions

In this paper, we have studied the local stability and local bifurcations for the reduced second-order system abstracted from Moore and Greitzer's third-order model. The stability conditions of system equilibrium are obtained by system linearization, while the existence conditions for the Andronov-Hopf bifurcation are derived via bifurcation theorem. Numerical simulations are obtained to verify the analytical results. It is concluded from those simulations that no surge behavior is observed for the compressor dynamics

with equilibrium point lying on either un-stalled normal zone or pre-stall zone. However, the deep-surge is found to occur on both two-dimensional reduced system and the original third-order Moore-Greitzer's model for the system equilibrium lying on the stall zone with large value of *B*-parameter. The analytical results and numerical simulations presented in this paper might provide an insight of the axial flow compression systems, which can give a guide in the control design for practical applications.

REFERENCES

[1] F.K. Moore, and E.M. Greitzer,, "A theory of post-stall transients in axial compression systems: part I-development of equations," *ASME J. Engineering for Gas Turbines and Power*, vol. 108, 1986, pp. 68-76.

[2] V.H. Garnier, A.H. Epstein, and E.M. Greitzer, "Rotating waves as a stall inception indication in axial compressors," *ASME J. Turbomachinery*, vol. 113, pp. 290-302,1991.

[3] E.M. Greitzer, "Surge and rotating stall in axial flow compressor: part I-theoretical compression system model," *ASME J. Engineering for Power*, vol. 98, 1976, pp. 190-198.

[4] F.E. McCaughan,, "Application of bifurcation theory to axial flow compressor instability," *ASME J. Turbomachinery*, vol. 111, 1989, pp. 426-433.

[5] D.-C. Liaw, and E.H. Abed, "Active control of compressor stall inception: a bifurcation theoretic approach," *Automatica*, vol. 32, 1996, pp. 109-115.

[6] M. F. W. Chowdhury, M. P. Schoen and J. Li, "Parameter identification and fuzzy logic controller design for a one-stage axial flow compressor system based on Moore-Greitzer model," *Proc. 2020 Intermountain Engineering, Technology and Computing (IETC)*, Orem, UT, USA., 2020.

[7] W. Si, F. Yang, W. Zeng and Q. Wang, "Modeling and detection of spike-type stall in axial compressors via deterministic learning theory," *Proc. 2016 Chinese Control and Decision Conference (CCDC)*, Yinchuan, China, 28-30 May 2016.

[8] P. Chen and H. Qin, "Bifurcation control of rotating stall in axial flow compressors via dynamic output feedback," *Proc. the 8th World Congress on Intelligent Control and Automation*, Jinan, China, July 6-9 2010.

[9] N. A. Chaturvedi and S. P. Bhat, "Output-Feedback semiglobal stabilization of stall dynamics for preventing hysteresis and surge in axial-flow compressors," *IEEE Trans. on Control Systems Technology*, vol. 14, NO. 2, March 2006, pp. 301-307.

[10] D.-C. Liaw, and J.–T. Huang, "Fuzzy control for stall recovery of axial-flow compressor dynamics," *Journal of Control Systems and Technology*, vol. 6, 1998, pp. 231-241.

[11] D.-C. Liaw, and J.-T. Huang,, "Robust stabilization of axial flow compressor dynamics via sliding mode design," *ASME Journal of Dynamic Systems, Measurement, and Control*, vol. 123, 1998, pp. 488-495.

[12] D.-C. Liaw, Y.-H. Huang, and W.-C. Chung, "Linear state feedback design for surge control of axial flow compressor dynamics," *Journal of Marine Science and Technology*, vol. 22, 2014, pp. 352-361.

[13] D.-C. Liaw, C.-C. Song, and J.-T. Huang, "Robust stabilization of a centrifugal compressor with spool dynamics," *IEEE Trans. on Control Systems Technology*, vol. 12, 2004, pp. 966-972.

[14] E.J. Doedel, "AUTO: A program for the automatic bifurcation analysis of autonomous systems," *Congressus Numerantium*, vol. 30, 1981, pp. 265-284.

[15] E.J. Doedel, A.R. Champneys, T.F. Fairgrieve, Y.A. Kuznetsov, B. Sandstede, and X. Wang, *AUTO 97: Continuation and bifurcation software for ordinary differential equations*, Computer Science Dept., Concordia Univ., 1998.

[16] D.-C. Liaw, W.-C. Lee, S.-M. Ren, and Y.-Y. Tsay, "A parametric study of axial flow compressor dynamics," *Proc. the 4th Pacific International Conference on Aerospace Science and Technology*, Kaohsiung Taiwan, 2001.

[17] G. Iooss, and D.D. Joseph,, *Elementary Stability and Bifurcation Theory*. 2nd Ed., Springer-Verlag, New York, 1990.

Der-Cherng Liaw, Institute of Electrical and Control Engineering, National Yang Ming Chiao Tung University, 1001 Ta Hsueh Road, Hsinchu, Taiwan, R.O.C.

Li-Feng Tsai, Institute of Electrical and Control Engineering, National Yang Ming Chiao Tung University, 1001 Ta Hsueh Road, Hsinchu, Taiwan, R.O.C.

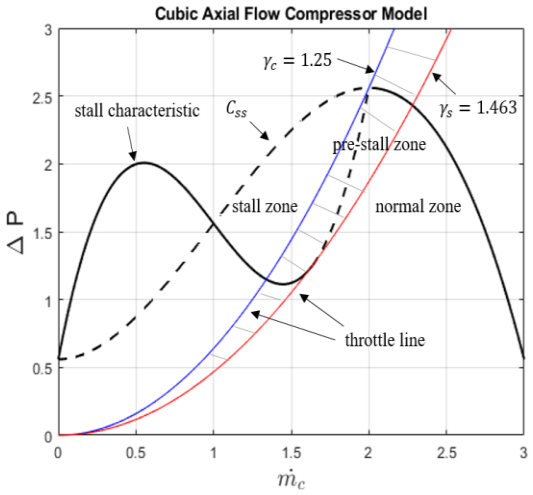

Fig. 1. A cubic axial flow compressor model

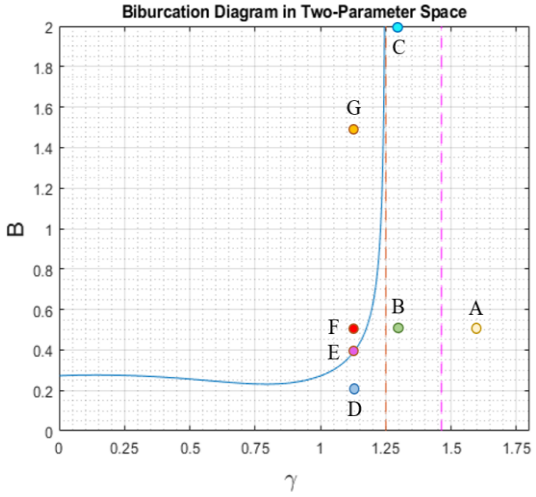

Fig. 2. Two-parameter bifurcation diagram of the reduced Moore and Greitzer's model

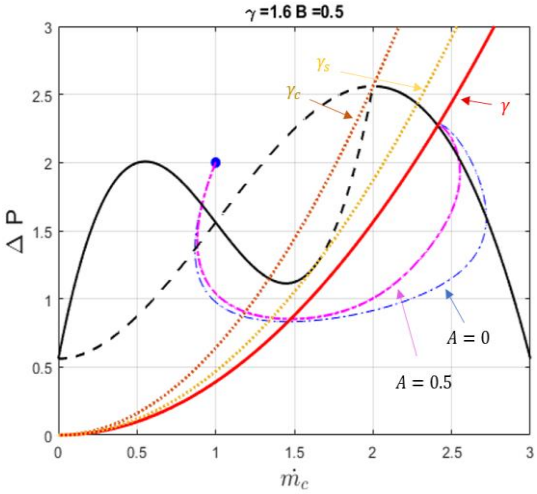

Fig. 3. Time response of ΔP vs. $\dot{m}_C$ in the normal un-stalled zone

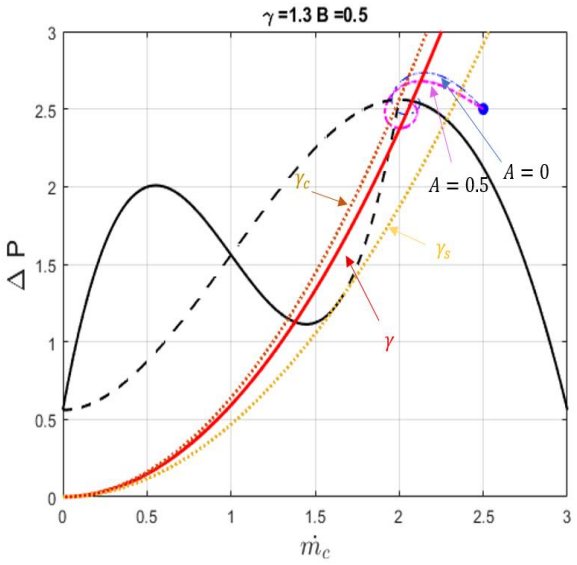

Fig. 4. Time response of ΔP vs. $\dot{m}_C$ in the pre-stall zone for small B-value with initial close to high pressure equilibrium point

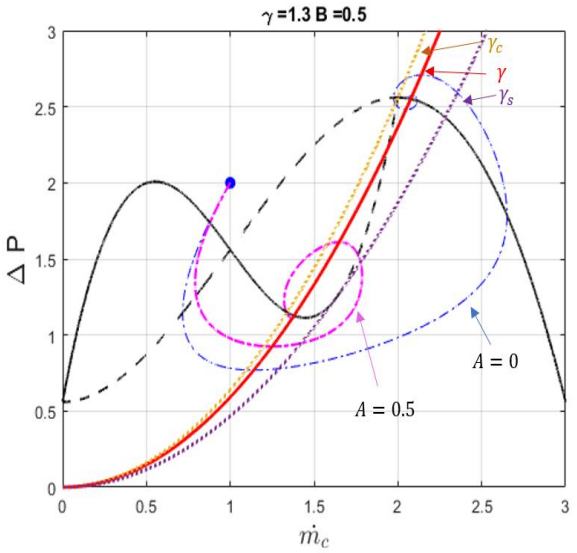

Fig. 5. Time response of ΔP vs. $\dot{m}_C$ in the pre-stall zone for small B-value with initial close to low pressure equilibrium point

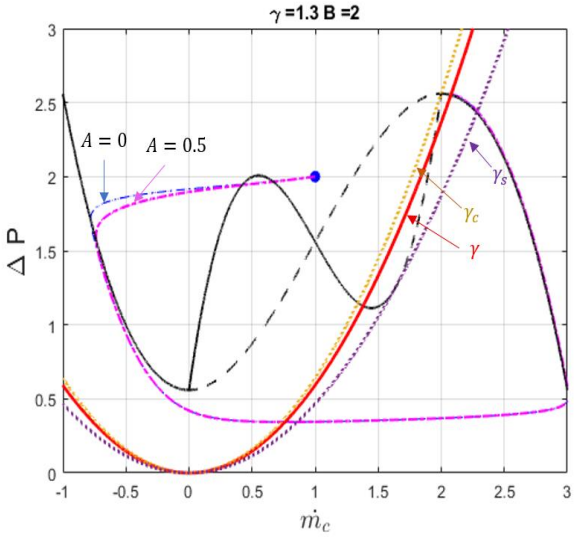

Fig. 6. Time response of ΔP vs. $\dot{m}_C$ in the pre-stall zone for large B-value with initial close to high pressure equilibrium point

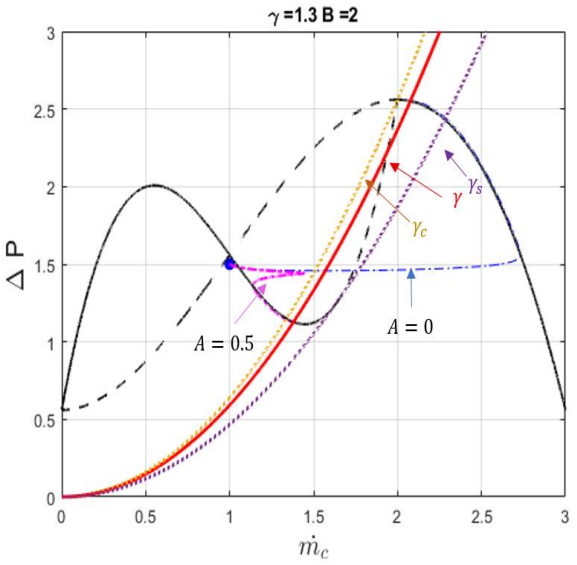

Fig. 7. Time response of ΔP vs. $\dot{m}_C$ in the pre-stall zone for large B-value with initial close to low pressure equilibrium point

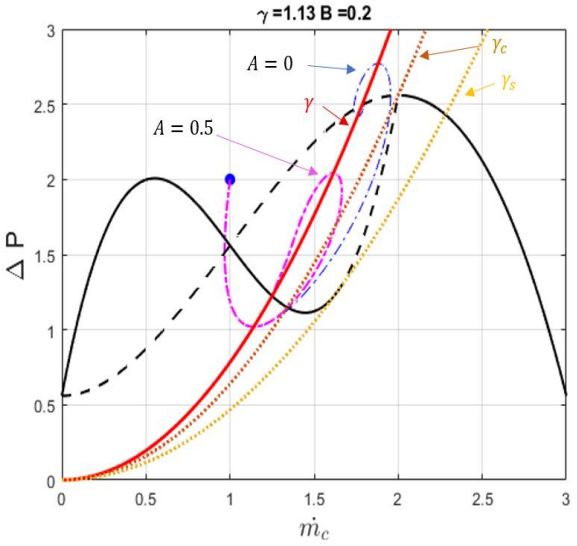

Fig. 8. Time response of ΔP vs. $\dot{m}_C$ in the stall zone for small B-value

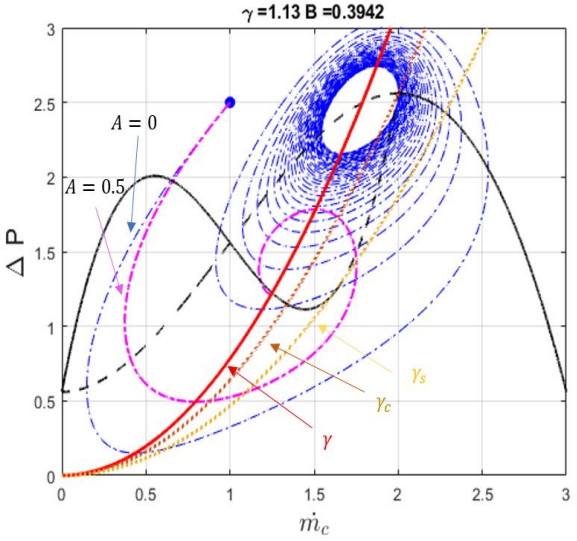

Fig. 9. Time response of ΔP vs. $\dot{m}_C$ in the stall zone for medium B-value (at Andronov-Hopf bifurcation point)

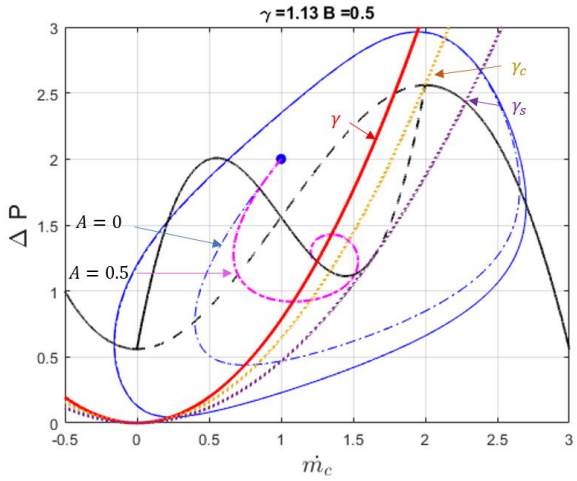

Fig. 10. Time response of ΔP vs. $\dot{m}_C$ in the stall zone for medium B-value (surge behavior)

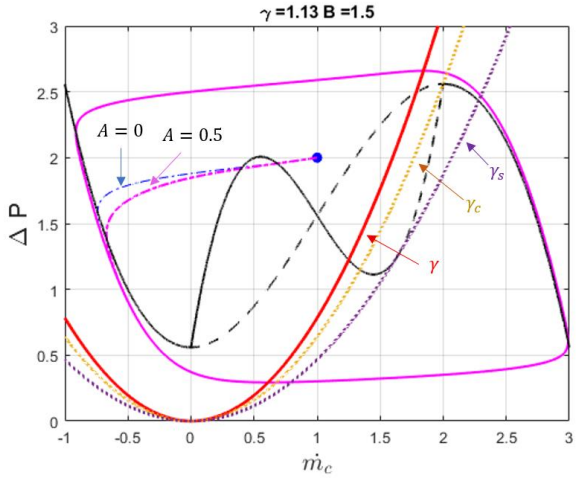

Fig. 11. Time response of ΔP vs. $\dot{m}_C$ in the stall zone for large B-value (deep surge)